Determination of Gradient-Elastic Constants in Cubic Solids

H. J. HACKELOER * and O. KANERT *

Physikalisches Institut der Universität Münster

(Z. Naturforsch. **27 a**, 1235—1239 [1972]; received 23 May 1972)

The effect of static elastic stress on the NMR signal in $LiCl^{35}$, $Rb^{85}Cl^{35}$, and $Rb^{87}Br$ is used to determine the gradient elastic constants relating the electric field gradient at the given nucleus to the elastic deformation. In contrast to previous experiments the quadrupole distortion produced by internal lattice distortion (point defects, dislocations etc.) is considered. Neglecting these distortions leads to an error in the determination of the gradient elastic constants by an order of magnitude.

I. Introduction

In a strain-free cubic crystal, the local electric field gradients (EFG) vanish at the nuclear sites because of the cubic point symmetry of the lattice. However, an uniaxial stress acting in a given direction on the crystal lowers the symmetry and produces a constant EFG-Tensor $\{V_{ik}\}$ at the site of any nucleus in the lattice resulting in a quadrupole distortion for a nuclear spin $I>1/2$. In the elastic region i. e. for a sufficiently small stress the EFG-tensor is a linear function of stress and strain respectively as shown by SHULMAN et al. [1]. In a cubic lattice, the corresponding fourth rank tensor connecting the field gradients $\{V_{ik}\}$ with the stress components $\{\sigma_{ik}\}$ possesses only two independent matrix elements C_{11} and C_{44} (Voigt notation). In terms of these elements the field gradients can be written as:

$$\begin{aligned} V_{x_1x_1} &= C_{11}\left(\sigma_{x_1x_1} - \tfrac{1}{2}\left(\sigma_{x_2x_2}+\sigma_{x_3x_3}\right)\right) \\ V_{x_1x_2} &= C_{44}\cdot\sigma_{x_1x_2} \end{aligned} \qquad (1)$$

(cyclic in the cubic axes $x_1=\langle 100\rangle$, $x_2=\langle 010\rangle$, $x_3=\langle 001\rangle$). Several experimental groups have used the quadrupole distortion of the NMR signal given by an external elastic stress in order to determine the two gradient-elastic constants for crystals with cubic point symmetry [2–7]. However, elastic strains in the crystal can also be produced by internal lattice defects. In this case, the assumption of an ideal crystal is not valid. This paper expands the relations given by SHULMAN [1] and LEMANOV [2] to a cubic crystal distorted by internal strains. This is always the case in real crystals, since only a few types of single crystals can be produced free of lattice defects. Using these modified relations, gradient elastic constants of Cl^{35} and Rb^{87} in RbCl, RbBr and LiCl single crystals distorted by internal lattice defects are determined by NMR-measurements.

* Present address: Institut für Physik der Universität Dortmund, *D-4600 Dortmund-Hombruch.*

II. Theory

In general, the shape $g(\omega)$ of the NMR line of nuclei with spin $I>1/2$ resulting from n mutually independent line broadening effects, each of which characterized by a normalized distribution function $g_i(\omega)$ can be written as

$$g(\omega)=\sum_{m=-I}^{I-1} c_m\left(g_1^{(m)}(\omega)\oplus g_2^{(m)}(\omega)\oplus\ldots\oplus g_n^{(m)}(\omega)\right) \qquad (2)$$

where c_m is the relative transition probability $m\to m+1$

$$c_m=\frac{I(I+1)-m(m+1)}{\sum_{m=-I}^{I-1}\left[I(I+1)-m(m+1)\right]}$$

and $\oplus$ stands for convolution.

In the case of a rigid cubic lattice distorted by lattice defects and an external uniaxial stress the distribution functions $g_i^{(m)}(\omega)$ are given by

1) the magnetic dipole interaction of nuclear spins, which is independent of the spin quantum number m: $g_1^{(m)}(\omega)=g_D(\omega)$;
2) the electric quadrupole interaction between the nuclear quadrupole moment Q and the local EFG given by the lattice defects:
$$g_2^{(m)}(\omega)=g_Q^{(m)}(\omega);$$
3) the electric quadrupole interaction between the quadrupole moment Q and the constant EFG caused by the external stress σ_0:
$$g_3^{(m)}(\omega)=\delta(\omega-\omega_\sigma^{(m)}).$$

Dieses Werk wurde im Jahr 2013 vom Verlag Zeitschrift für Naturforschung in Zusammenarbeit mit der Max-Planck-Gesellschaft zur Förderung der Wissenschaften e.V. digitalisiert und unter folgender Lizenz veröffentlicht: Creative Commons Namensnennung-Keine Bearbeitung 3.0 Deutschland Lizenz.

This work has been digitalized and published in 2013 by Verlag Zeitschrift für Naturforschung in cooperation with the Max Planck Society for the Advancement of Science under a Creative Commons Attribution-NoDerivs 3.0 Germany License.

Zum 01.01.2015 ist eine Anpassung der Lizenzbedingungen (Entfall der Creative Commons Lizenzbedingung „Keine Bearbeitung") beabsichtigt, um eine Nachnutzung auch im Rahmen zukünftiger wissenschaftlicher Nutzungsformen zu ermöglichen.

On 01.01.2015 it is planned to change the License Conditions (the removal of the Creative Commons License condition "no derivative works"). This is to allow reuse in the area of future scientific usage.

In first order perturbation the resulting elastic quadrupole frequency shift $\omega_\sigma^{(m)}$ can be expressed as

$$\omega_\sigma^{(m)} = (2\,m+1)\,\frac{3\,e\,Q}{4\,I(2\,I-1)\,\hbar}\cdot V_{zz}^{(\sigma)} = (2\,m+1)\,a_\sigma \tag{3}$$

where $V_{zz}^{(\sigma)}$ is the component of the EFG tensor $\{V_{ik}\}$ in the direction of the applied magnetic field H_0 caused by the external load σ_0.

As shown by LEMANOV [2], the correlation between the stress σ_0 acting in the x-direction of the laboratory frame (x, y, z parallel to H_0) and the EFG $V_{zz}^{(\sigma)}$ depends on the direction of the stress σ_0 with respect to the crystal axes as follows:

1) σ_0 parallel to $\langle 100\rangle$

$$V_{zz}^{(\sigma)} = -\frac{C_{11}}{2}\cdot\sigma_0; \tag{4a}$$

2) σ_0 parallel to $\langle 110\rangle$

$$V_{zz}^{(\sigma)} = -\frac{\sigma_0}{4}\left(\frac{C_{11}}{2}+C_{44}+\cos 2\,\varphi\,(\tfrac{3}{2}\,C_{11}-C_{44})\right) \tag{4b}$$

3) σ_0 parallel to $\langle 111\rangle$

$$V_{zz}^{(\sigma)} = -\frac{C_{44}}{3}\cdot\sigma_0. \tag{4c}$$

Here φ is the angle between the static magnetic field H_0 (z-direction) and the crystal axis $\langle 001\rangle$.

Now Eq. (2) can be rearranged as

$$g(\omega) = c_{-1/2}\,g_D(\omega) + \sum_{m=1/2}^{I-1} 2\,c_m\cdot g_D(\omega)\oplus g_Q^{(m)}\,(\omega-\omega_\sigma^{(m)}). \tag{5}$$

Assuming a Gaussian line shape for the dipolar function $g_D(\omega)$ as well as for the quadrupole function $g_Q^{(m)}(\omega) = g_Q((2\,m+1)\,a)$ (see: GRAVELY and MEMORY [8] and KANERT and MEHRING [9]) one can write

$$g_D(\omega) = \frac{1}{\sqrt{2\,\pi}}\cdot\frac{1}{\Delta}\cdot\exp\left(-\frac{\omega^2}{2\,\Delta^2}\right) \tag{6a}$$

and

$$g_Q^{(m)}(\omega) = \frac{1}{\sqrt{2\,\pi}}\cdot\frac{1}{(2\,m+1)\langle a^2\rangle^{1/2}}\cdot\exp\left(-\frac{\omega^2}{(2\,m+1)^2\langle a^2\rangle}\right). \tag{6b}$$

Here Δ^2 is the dipolar second moment given by VAN VLECK's formula [10], $\langle a^2\rangle$ is the second moment of the distribution of quadrupole frequencies

$$a(\boldsymbol{r}) = \frac{3\,e\,Q}{4\,I(2\,I-1)\,\hbar}\cdot V_{zz}(\boldsymbol{r}) \tag{7}$$

determined by the local distribution of the component $V_{zz}(\boldsymbol{r})$ of the EFG-Tensor caused by the lattice defects. Using the normalized frequency $\Omega = \omega/\Delta$, the normalized internal mean quadrupole distortion $w = \langle a^2\rangle^{1/2}/\Delta$, and the normalized external quadrupole perturbation $w_\sigma = a_\sigma/\Delta$ one can write the normalized representation of Eq. (5) as shown by KANERT and MEHRING [9] as

$$g(\Omega) = \frac{c_{-1/2}}{\sqrt{2\,\pi}}\cdot\exp\left(\frac{-\Omega^2}{2}\right) + \sum_{m=1/2}^{I-1}\frac{1}{(1+(2\,m+1)^2\cdot w^2)^{1/2}}\cdot\exp\left\{-\frac{\Omega^2+(2\,m+1)^2\,w_\sigma^2}{2\,(1+(2\,m+1)^2\,w^2)}\right\}\cdot\cosh\frac{(2\,m+1)\,w_\sigma\cdot\Omega}{1+(2\,m+1)^2\cdot w^2}. \tag{8}$$

Starting from the derivative $f(\Omega) = (\mathrm{d}/\mathrm{d}\Omega)\cdot g(\Omega)$ of Eq. (8), which is actually recorded in NMR wide-line experiments, the relative peak intensity f_m/f_{m_0} can be calculated as a function of the two parameters w and w_σ respectively.

An analytical expression is given only in the case of an ideal crystal and of a small frequency shift a_σ, i. e. $w = 0$, $(2\,m+1)\cdot w_\sigma \ll 1$. The result

$$f_m/f_{m_0} = 1 - 3\,w_\sigma^2\sum_{m=1/2}^{I-1}(2\,m+1)^2\cdot c_m$$

differs from the formula

$$f_m/f_{m_0} = 1 - 2\,w_\sigma^2\,(2\,m+1)^2\cdot\sum_{m=1/2}^{I-1} c_m$$

derived in a simple way by LEMANOV [2]. The reason for this is the incorrect weighting of the several satellite transitions in the second equation and the rough calculation of the peak intensity by means of second moments. Generally, the function $f(\Omega)$ and the peak intensity f_m/f_{m_0} were calculated numerically by means of a computer IBM 360/50. Some typical results of those calculations are plotted in Fig. 1 for a spin $I = 3/2$. The upper picture in Fig. 1 demonstrates the behaviour of the derivative $f(\Omega)$ of the wide-line signal for three different sets of internal and external distortion parameters w and w_σ. For certain values of those parameters the appearence of two maxima for $\Omega \gtrless 0$ due to the undisturbed central transition $1/2 \rightarrow -1/2$ and the satellite transition $\pm 3/2 \longleftrightarrow \pm\,\frac{1}{2}$ shifted by the frequency a_σ is evident. The lower picture in Fig. 1 shows the behaviour of the peak intensity f_m/f_{m_0} for several values of the internal distortion parameter w ($w = 0$; 0,5; 1) as a function of the external quadrupole distortion w_σ.

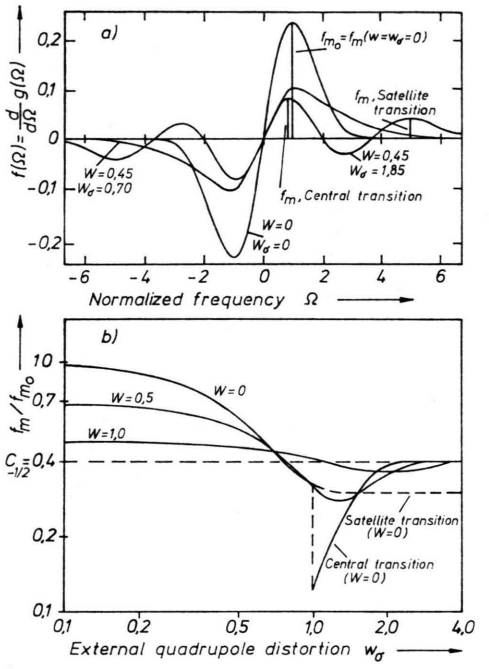

Fig. 1. a) Theoretical line shape of the NMR wide-line signal $f(\Omega)=\frac{d}{d\Omega}g(\Omega)$ for three different cases of internal and external quadrupole distortion parameters w, w_σ. b) Calculated peak intensity f_m/f_{m_0} of the wide-line signal $f(\Omega)$ versus external quadrupole distortion w_σ. Parameter: Normalized internal quadrupole distortion w [see Eq. (8)]. Nuclear spin $I=3/2$.

As expected for small values of w_σ the peak intensity f_m/f_{m_0} decreases monotonically with increasing perturbation w_σ. However the variation of f_m/f_{m_0} as a function of w_σ depends extremely on the internal quadrupole distortion w of the crystal. In consequence the error in the determination of the gradient-elastic constants would be large without considering the internal strains in the sample. As discussed before, for sufficiently large values of w_σ two maxima in the function $f(\Omega)$ appeared for $\Omega \gtrless 0$. This leads to a discontinuity in the behaviour of the peak intensity f_m/f_{m_0} for $w=0$ at $w_\sigma=1$: The dashed line shows the variation of the peak intensity of the outer satellite transition with w_σ, whereas the solid line represents the variation of the inner peak intensity with w_σ. For the cases $w=0.5$; $w=1.0$ only the height f_m/f_{m_0} for the first maximum is drawn in Figure 1 b. As a consequence of first order quadrupole perturbation theory all curves in the figure converge asymptotically against the relative intensity $c_{-1/2}=0.4$ of the central transition.

III. Experimental Details

Single crystals of RbCl, RbBr and LiCl were oriented grown in an inert gas (Ar) by the Czochralski method from chemical super pure material supplied by Merck, Darmstadt, Germany. Every crystal was polished to a cylindrical sample of about 15 mm diameter and 25 mm length with a cylinder axis parallel to the $\langle 100\rangle$- and $\langle 110\rangle$-direction, respectively. The crystals were elastically deformed using a simple pressure device consisting of a piston with a lever arm and a counterpart assembly mounted inside the gap of the electromagnet. To avoid non-uniaxial stress components, the piston and counterpart were accurately machined and the faces of the sample were coated with a cap of hard plastic material, which could be machined to fit into the pressure device. Since LiCl is very hygroscopic, these crystals were protected by paraffin oil during the measurements. The external pressure, produced by several weights hanging on the end of the lever arm acts along the cylinder axis of the sample, perpendicular to the applied magnetic field H_0. Two sets of measurements were carried out in order to determine the gradient-elastic constants C_{11} and C_{44}:

1) σ_0 parallel to $\langle 100\rangle$, H_0 parallel to $\langle 001\rangle$ [Eq. (4 a)],
2) σ_0 parallel to $\langle 110\rangle$, H_0 parallel to $\langle \bar{1}10\rangle$ [$\varphi=90°$, Eq. (4 b)].

The NMR measurements were performed with a conventional wide-line spectrometer including an automatic controlled twin T-bridge described elsewhere [11]. The resonant frequency was 5.5 Mc for Cl^{35} and 14 Mc for Rb^{87}, respectively. To eliminate long time drifts all measurements were referred to a standard sample measurement.

In order to obtain the peak intensity f_{m0} corresponding to the strain-free crystal, after the elastic measurements every sample was plastically deformed strong enough to reach the peak intensity of $c_{-1/2}\cdot f_{m0}=0.4\,f_{m0}$ ($I=\frac{3}{2}$), produced by the central transition only.

IV. Results and Discussion

Figure 2 shows an example of the measured peak intensity f_m/f_{m_0} of Cl^{35} in a LiCl single crystal as a function of the external quadrupole distortion w_σ with σ_0 parallel to $\langle 100\rangle$ and H_0 parallel to $\langle 001\rangle$. The value $f_m/f_{m_0}(w_\sigma=0)=0.719$ leads to an internal distortion parameter of $w=0.45$, which differs from zero in a pronounced manner. The theoretical curve given by the numerical evaluations of Eq. (8) was fitted to the measurements with $C_{11}=1.5\cdot 10^3$ dyne$^{-1/2}$, using $\Delta=6.8\cdot 10^2$ sec^{-1} for the dipolar width. As seen in the figure the agreement between the measurements and the theory is quite well.

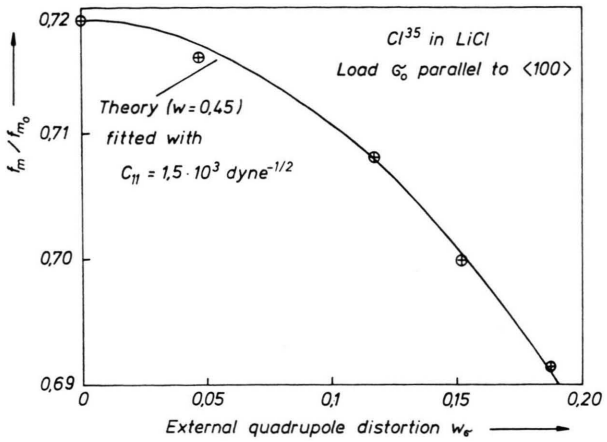

Fig. 2. Normalized peak intensity f_m/f_{m_0} of the Cl^{35}-signal in a LiCl single crystal as a function of the external quadrupole distortion w_σ. External stress σ_0 parallel to ⟨100⟩, magnetic field H_0 parallel to ⟨001⟩. The measurements were fitted with the theoretical curve [Eq. (8)] and $C_{11}=1.5\cdot10^3$ dyne$^{-1/2}$.

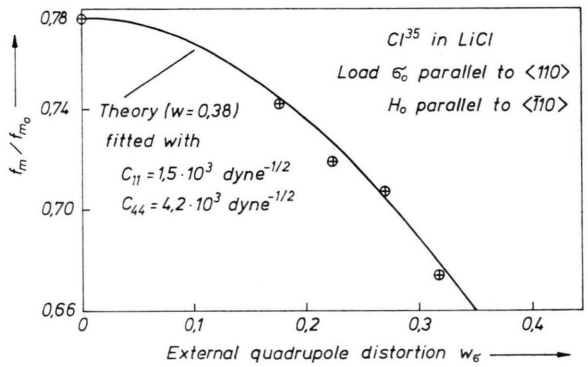

Fig. 3. Normalized peak intensity f_m/f_{m_0} versus w_σ for Cl^{35} in a different sample of LiCl, with σ_0 parallel to ⟨110⟩ and H_0 parallel to ⟨$\bar{1}$10⟩. The line fit analogous to Fig. 2 results in $C_{44}=4.2\cdot10^3$ dyne$^{-1/2}$ by using the value of C_{11} as obtained from Figure 2.

Figure 3 shows a corresponding measurement on a different sample for H_0 parallel to ⟨$\bar{1}$10⟩ and σ_0 parallel to ⟨110⟩. The curve was fitted to the experimental points by using Equation (4 b) with $\Delta = 4.9\cdot10^2$ sec^{-1} and the constant $C_{11}=1.5\cdot10^3$ dyne$^{-1/2}$ as obtained from Fig. 2 and $w=0.38$. This leads to the evaluation of C_{44}. Using the dipolar second moment Δ, the quadrupole frequency a_σ was determined from Figs. 2 and 3 as a function of the external stress σ_0 and plotted in Figure 4. As expected from Eqs. (4 a) – (4 c), (7) a linear relation holds for a_σ versus σ. Gradient-elastic constants for several alkali halides, as obtained in the described manner are summarized in Table 1. Instead of the gradient-elastic constants C_{11}, C_{44} the constants S_{11}, S_{44} can be introduced, which connect the electric field gradient $\{V_{ik}\}$ with the elastic strain $\{\varepsilon_{ik}\}$. A simple relation can be obtained as follows [9]:

$$C_{11} = (s_{11} - s_{12})\, S_{11}\,, \qquad C_{44} = s_{44}\, S_{44}$$

where the s_{ik} are the elastic compliance constants.

Nucleus	Crystal	C_{11} dyne$^{-1/2}$	C_{44} dyne$^{-1/2}$	S_{11} dyne$^{1/2}$cm^{-2}	S_{44} dyne$^{1/2}$cm^{-2}	Error
Cl^{35}	LiCl	$1{,}5\cdot10^3$	$4{,}2\cdot10^3$	$4{,}1\cdot10^{14}$	$10{,}4\cdot10^{14}$	±20%
Cl^{35}	RbCl	$2{,}2\cdot10^3$	$4{,}9\cdot10^3$	$6{,}6\cdot10^{14}$	$2{,}3\cdot10^{14}$	±30%
Rb^{87}	RbCl	$9{,}7\cdot10^3$	$15{,}3\cdot10^3$	$29{,}1\cdot10^{14}$	$7{,}4\cdot10^{14}$	±30%
Rb^{87}	RbBr	$6{,}5\cdot10^3$	$16{,}0\cdot10^3$	$17{,}3\cdot10^{14}$	$6{,}1\cdot10^{14}$	±30%

The quoted errors in Table 1 are due to the following experimental and theoretical ambiguities:

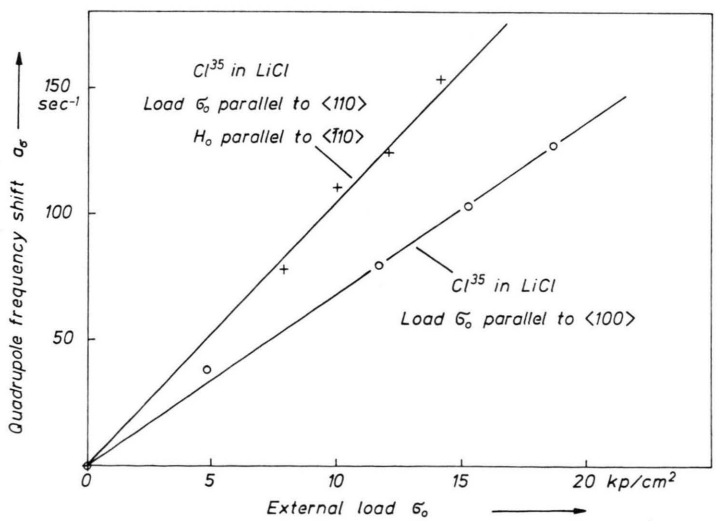

Fig. 4. The quadrupole frequency a_σ versus the external stress σ_0 calculated from Figs. 2 and 3 for the two different directions of σ_0 and H_0 with respect to the crystal axes. As expected theoretically it results in a straight line [Eqs. (4 a)–(4 c), (7)].

1) Error in the measurement of the peak intensity f_m as the function of the external stress σ.
2) Error in the determination of the corresponding intensity f_{m_0} of the strain-free crystal.
3) Error in the experimental determination of the dipolar width Δ.
4) Incorrect assumption of Gaussian line shape for the dipolar and quadrupolar broadening function [12].

Acknowledgements

The authors would like to thank Prof. Dr. M. MEHRING for useful discussions.

[1] R. G. SHULMAN, B. J. WYLUDA, and P. W. ANDERSON, Phys. Rev. **107**, 953 [1957].
[2] V. V. LEMANOV, Soviet Phys. JETP **13**, 543 [1961].
[3] J. L. MARSH and P. A. CASABELLA, Phys. Rev. **150**, 546 [1966].
[4] V. L. BOGDANOV and V. V. LEMANOV, Soviet Phys. Sol. State **10**, 159 [1968].
[5] R. W. ASTRUE and H. O. HOOPER, Phys. Rev. **164**, 1206 [1967].
[6] Y. A. GRINCHENKO, E. R. DOBROVINSKAYA, and V. L. TIMAN, Sov. Phys. Sol. State **10**, 341 [1968].
[7] O. KANERT, Phys. Stat. Sol. **32**, 667 [1969].
[8] B. T. GRAVELY and I. D. MEMORY, Phys. Rev. **3 B**, 3426 [1971].
[9] O. KANERT and M. MEHRING, Static Quadrupole Effects in Disordered Cubic Solids, Springer-Verlag, Berlin 1971.
[10] J. H. VAN VLECK, Phys. Rev. **74**, 1168 [1948].
[11] M. MEHRING and O. KANERT, Rev. Sci. Instrum. **42**, 449 [1965].
[12] O. KANERT, D. KOTZUR, and M. MEHRING, Phys. Stat. Sol. **36**, 291 [1969].

Monte-Carlo-Rechnung für die Streuung von keV-Ionen an polykristallinen Stoffen

G. BETZ

II. Institut für Experimentalphysik, Technische Hochschule, Wien

(Z. Naturforsch. **27 a**, 1239—1246 [1972]; eingegangen am 3. Juni 1972)

Monte-Carlo-Calculation for the Backscattering of keV-ions at Polycrystalline Solids

Assuming a random distribution of the target atoms and taking account of electronic stopping too, the Monte-Carlo technique, based on a single collision model, was used to simulate the scattering of keV-ions at polycrystalline solids. The reflection coefficient, angular and energy distribution and penetration depth of the reflected particles have been calculated for various ion-target combinations and energies. Furtheron, the angle of incidence of the primary beam was varied. Calculated values of the reflection coefficient and its dependence on angle of incidence are found in good agreement with experimental results. The percentage of particles scattered after a given number of collisions was also investigated.

I. Einleitung

Die Streuung von keV-Ionen an polykristallinen Festkörperoberflächen hat in den letzten Jahren großes Interesse gefunden, unter anderem auch als Methode zur Oberflächenanalyse [1]. Verschiedene Methoden zur Berechnung der Streuung sehr leichter Ionen an Festkörperoberflächen wurden entwickelt [2–4].

Ausgehend von der LINDHARD-SCHARFF-SCHIØTT-Theorie [5] über die Wechselwirkung von energetischen Ionen mit Festkörpern und den Berechnungen von WINTERBON et al. [6] haben BØTTIGER, DAVIES, SIGMUND und WINTERBON [7] Streukoeffizienten für verschiedene Ion-Targetkombinationen aus Berechnungen über die Abbremsung von Ionen in einem unendlich ausgedehnten, isotropen Medium erhalten.

Sonderdruckanforderungen an Prof. Dr. F. P. VIEHBÖCK, II. Institut für Experimentalphysik, Technische Hochschule Wien, *A-1040 Wien*/Österreich, Karlsplatz 13.

Für die Untersuchung von Streuprozessen erweist sich auch die Monte-Carlo-Methode als sehr geeignet. Sie wurde bereits von verschiedenen Autoren für die Berechnung der Reichweite von Ionen in Festkörpern [8, 9], für die Berechnung des Zerstäubungskoeffizienten [10, 11] bei Ionenbeschuß und für die Streuung von MeV-Ionen [12] und sehr leichten Ionen [13] an Festkörperoberflächen verwendet.

In der vorliegenden Arbeit wird die Streuung von keV-Ionen an Festkörperoberflächen ebenfalls mit Hilfe der Monte-Carlo-Methode untersucht. Unter der Annahme einer isotropen Verteilung der Targetatome und Beschränkung auf 2-Teilchenstöße wird die Bahn eines einfallenden Ions im Target gemäß der Monte-Carlo-Methode verfolgt. Neben elastischen Energieverlusten durch Stöße des Primärteilchens mit Targetatomen werden auch kontinuierliche Energieverluste durch Elektronenanregung berücksichtigt. Die berechneten Streukoeffizienten und ihre Abhän-